

# Optimisation of BLDC motors for Drone Applications

Christopher Vail

## Abstract

Motor selection is a key part of any drone design - matching the power required to drive the propeller while keeping the motor itself as light as possible is critical. Typically, propellers require low torque and high RPM for peak performance [1]. Aside from the battery, the four motors required in a quad-copter are a significant contributor to the overall weight and as such the overarching efficiency. This paper seeks to find an optimal motor design which satisfies the requirements to generate sufficient thrust for the drone while minimising the mass.

The model developed consisted of 8 design variables and 6 design parameters. By setting the design parameters to appropriate values and correctly bounding the design space the optimised variables for a BLDC motor are calculated. The optimisation methodology is robust and efficient, using a GA-SQP pipeline to quickly sample and converge to a globally optimal solution. Further development of complex loss equations for hysteresis and cogging are required to gain reliable insights into the efficiency of the optimised solution.

## 1 Model Development

Figure 1 shows a cross section of a typical BLDC motor from which the objective function was derived. The mass was calculated by splitting the various parts into simplified shapes (rectangles, cylinders and hollow cylinders) which were then multiplied by the respective height and density to develop an equation for the overall motor weight.

### 1.1 Torque Equation

To calculate the torque produced by the motor first the force produced by a single tooth was considered.

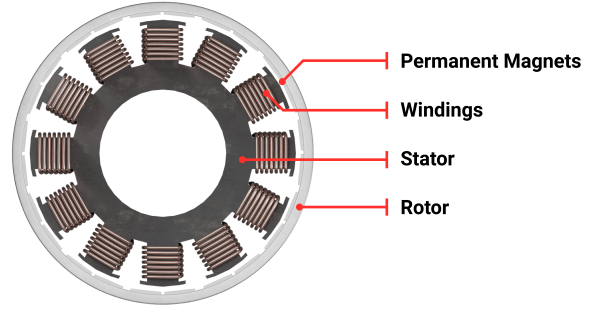


Figure 1: Cross-section of a typical BLDC out-runner motor

The force produced by a coil of wire acting in a  $\beta$  field is given by:

$$F = I\vec{L} \times \beta \quad (1)$$

The laminated iron core of the tooth focuses the magnetic field produced by all the coil windings. Additionally it reduces the size of eddy currents produced. As the stator radius is much larger than the air gap, all components can be assumed to be perpendicular meaning it is possible to simplify to the scalar equation. Assuming the winding length is approximately the perimeter of the tooth multiplied by the number of windings, Equation 1 defines the winding length.

$$L_w = 2(w_t + h_s) \quad (2)$$

Multiplying Equation 1 by the acting radius,  $r_s$ , and combining Equation 2 results in the torque equation.

$$\tau = \beta I L_w r_s \quad (3)$$

The  $\beta$  field at the stator is dependant on the air gap between the magnets and the stator and the magnet thickness. Equation 4 is used to adjust for this.

$$\beta_s = \frac{\beta_0 t_m}{t_m + t_{ag}} \quad (4)$$

To calculate the maximum current the motor could use a standard table of maximum operating current for winding wires was used. A polynomial curve was fitted across the design space with an  $R^2$  value of 1.00. The maximum operating current can then be given by Equation 5 where  $I_{max}$  is the batteries max current draw per motor.

$$I_{op} = \min(8.73 \cdot 10^6 r_w^2 + 281 r_w - 0.0428, I_{max}) \quad (5)$$

Substituting Equations 4 and 5 into Equation 3 results in the final equation for maximum motor torque.

$$\tau = \beta_s I_{op} L_w r_s \quad (6)$$

## 1.2 Power Equation

An electric motor, almost by definition, acts as a transducer; converting electrical energy into mechanical work. However, the conversion cannot be 100% efficient as undesirable energy is produced as heat among other sources. Equation 7 was developed by considering the power within the system.

$$IV = \tau\omega + I^2 R \quad (7)$$

The mechanical power produced ( $\tau\omega$ ), is summed with the losses which, in this simplified case, only contain the copper losses ( $I^2 R$ ). While some literature suggest that this is the most significant loss factor [1] they primarily discuss motors much larger than typically used in drones. Consideration of hysteresis and cogging losses are required for a more robust model. Friction in the bearings is considered negligible compared to the copper losses.

The current required to drive a propeller at a given torque and angular velocity can then be derived using the quadratic formula.

$$RI^2 - VI + \tau\omega = 0 \quad (8)$$

$$I = \frac{V - \sqrt{V^2 - 4R\tau\omega}}{2R} \quad (9)$$

The lower root of this quadratic is taken as it corresponds to the highest efficiency solution for that mechanical output. The higher root is found once the copper losses outstrip the mechanical power output. Currents this high should be avoided during any operation of a motor.

The resistance used in the Equations 7 - 9 is the winding resistance of the motor. This is calculated using the resistivity equation.

$$R = \frac{\rho L}{A} \quad (10)$$

Substituting values in for the resistivity of copper at 75°C as is convention, the wire radius and the winding length described in Equation 2, Equation 10 becomes:

$$R = \frac{\rho_c L_w}{\pi r_w^2} \quad (11)$$

To ensure sufficient mechanical power can be generated, the operating current developed in Equation 5 must be greater than the current developed in Equation 9.

## 1.3 Geometric Constraints

To design a physically feasible motor, a couple of geometric constraints were required. The first ensures that the width of the stator teeth at their inner radius is physically possible. The second is used to calculate the number of possible windings per tooth that could be wound.

### Tooth width constraint

The shaft, bearings and other internal aspects of a motor mean that the stator teeth can occupy only a fraction of the cylinder encompassed by the stator radius. For simplicity, it was assumed stator teeth could occupy  $0.6r_s$ . The perimeter at the inner radius of the tooth profile is then given by:

$$p_i = \pi(0.4r_s)^2 \quad (12)$$

The total tooth width at this radius is given by:

$$w_{total} = 3n_t w_t \quad (13)$$

Where  $n_t$  is the number of teeth per phase, giving rise to the factor of 3. The total tooth width must be less than the inner perimeter.

### Winding constraint

Practical knowledge suggests that beyond 3 winding layers, the flux linkage between the core and the winding starts to deteriorate. As such only up to 3 layers of wire was considered. Figure 2 shows the geometry of the problem.

Considering the 3 lines marked (Something), we first calculate the distance to either the  $r_0$  boundary or the

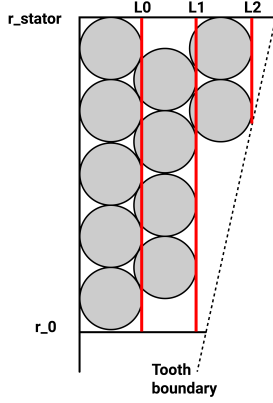


Figure 2: Winding Constraint Geometry

angled boundary for each line. Equation 14 calculates this distance where  $i$  is a counting variable ranging from 0 to 2.

$$r_i = \max\left(\frac{(0.5w_t + r_w + ir_w\sqrt{3})}{\tan\theta}, r_0\right) \leq 0 \quad (14)$$

The number of possible windings per layer can then be given by:

$$w_i = \text{floor}\left(\frac{r_s - r_i}{2r_w}\right) \quad (15)$$

Leading to the total number of windings possible expressed in Equation 16

$$w_{total} = \sum_{i=0}^2 w_i \quad (16)$$

#### 1.4 Assumptions

A number of assumptions have been made in order to arrive at the model developed. It was assumed that losses are primarily copper losses (Of the form  $I^2R$ ) as opposed to hysteresis losses or cogging effects. The mathematical formulation of the mentioned losses was too complex for the scope of this project. The book Electric Machinery 3<sup>rd</sup> edition [1] suggests this is an acceptable assumption but further review of literature for small BLDC motors is needed. The effects of cogging were mitigated by requiring at least 3 teeth per

phase.

Optimal magnetic conditions were also assumed, in so far as magnetic saturation of the core was ignored and perfect linkage between the wires and the core and the core and the magnets was assumed. This is reasonable as only 3 layers of windings per tooth were allowed. Edge effects of the  $\beta$  field were also discounted.

The structure of the optimisation script is designed such that the inclusion of further constraints is possible without significant refactoring of existing code.

To avoid having to use the limited number of optimisation methods available for non-linear constrained mixed integer programming problems, it was assumed that  $n_t$  and  $n_w$  could be modelled as continuous variables. Should an optimisation algorithm return non-integer values then the design space immediately surrounding will be explored and the best option chosen.

## 2 Model Analysis

### 2.1 Formalised Optimisation Problem

The equations opposite denote the negative null form of the optimisation problem described above. The optimisation is based on a set of design variables  $\vec{x}$  and parameters  $\vec{p}$  to minimise the motor mass,  $\vec{m}_{motor}$ .

### 2.2 Design Variables

The design variables cover the main defining factors in BLDC (Brushless DC) motor design. Firstly, with regards to stator design,  $n_t$  is the number of teeth per phase while  $w_t$  is the width of these teeth.  $h_s$  and  $r_s$  define the height and radius of the stator respectively which are the primary geometric variables in most motor designs. The number of coils of wire on the stator teeth is given by  $n_w$  and the wire radius is given by  $r_w$ . These are integral to the strength of the electromagnet and therefore the torque produced. Finally, the size of the air gap between the stator and rotor is given by  $t_{ag}$  and the thickness of the permanent magnets is  $t_m$ .

### 2.3 Design Parameters

For this optimisation problem the design parameters were assumed as follows. The maximum current draw from the battery was set to 5A at 12V. The cruising rpm and torque were set to 0.025 Nm and 11000 rpm respectively - requiring an output power of approximately 30W per propeller. To account for acceleration

it was assumed that torques as high as 5 times the cruising torque would be required. Finally N42 neodymium magnets were assumed which have a magnet remanence of approximately 1T.

### Optimisation Formula

$$\begin{aligned}
\min_{\vec{x}} \quad & f(\vec{x}, \vec{p}) = \|\vec{m}_{motor}\|_1 \\
\text{s.t.} \quad & \vec{x} = (n_w, n_t, w_t, h_s, r_s, r_w, t_{ag}, t_m)^T \\
& \vec{p} = (I_{max}, V, \tau_{cruise}, \omega_{cruise}, m_\tau, \beta_0)^T \\
& \vec{m}_{motor} = (m_t, m_w, m_{mag}, m_r, m_c)^T \\
& g_1 : 0.4\pi r_s - 3n_t w_t \leq 0 \\
& g_2 : n_w - \frac{1}{2r_w} \sum_{i=1}^3 r_s \\
& \quad - \max\left(\frac{(0.5w_t + r_w + ir_w\sqrt{3})}{\tan\theta}, r_0\right) \leq 0 \\
& g_3 : \frac{V - \sqrt{V^2 - 4R_w\tau_{cruise}\omega_{cruise}}}{2R_w} - I_{op} \leq 0 \\
& g_4 : m_\tau\tau_{cruise} - 4\beta_s I_{op}(2n_w n_t(2w_t + 2h_s))r_s \leq 0 \\
& h_1 : m_t - (w_t h_s (r_s 0.8 - 0.0025) + \\
& \quad 0.0025 h_s \cdot \left(\frac{2\pi r_s}{3n_w} - \frac{2\pi r_s}{200}\right))\rho_{LI} = 0 \\
& h_2 : m_w - \text{cyl}(r_w, n_t(2w_t + 2h_s), \rho_c) = 0 \\
& h_3 : m_{mag} - \text{hcy}(r_s + t_{ag}, r_s + t_{ag} + t_m, h_s, \rho_m) = 0 \\
& h_4 : m_r - \text{hcyl}(r_s + t_{ag} + t_m, r_s + t_{ag} + t_m 2, \\
& \quad h_s, \rho_{ms}) = 0 \\
& h_5 : m_c - 2\text{cyl}(r_s + t_{ag} + t_m 2, 1 \cdot 10^{-3}, \rho_c) = 0 \\
& h_6 : R_w - \frac{(2n_t n_w(2w_t + 2h_s))1.68_{10^{-6}}}{\pi r_w^2} = 0 \\
& h_7 : \beta_s - \frac{\beta_0 t_m}{t_{ag} + t_m} = 0 \\
& h_8 : I_{op} - \min(8.73 \cdot 10^6 r_w^2 + 281 r_w - 0.0428, \\
& \quad I_{max}) = 0 \\
& h_9 : \theta - \frac{\pi}{3n_t} = 0
\end{aligned}$$

### 2.4 Constraints

$g_1$  and  $g_2$  are geometric constraints to ensure feasible tooth widths based on the number of teeth and the stator radius as well as constraining the number of windings on the stator teeth.  $g_3$  limits the current required

Variable	$n_w$	$n_t$	$w_t$	$h_s$	$r_s$	$r_w$	$t_{ag}$	$t_m$
Upper Bound	inf	15	10	50	50	5	2	10
Lower Bound	5	3	2	10	10	0.08	0.4	2

Table 1: Upper and lower bounds of the design space

to drive the propeller to less than what either the battery can supply or the limiting current of the windings wire. Likewise,  $g_4$  ensures the motor can supply sufficient torque for all operating conditions. The upper and lower bounds of the design space have been omitted from this formulation for space. They are used to limit the design space to values that are physically possible and sensible. The values are outlined in Table 1.

### 2.5 Monotonicity Analysis

The thickness of the air gap,  $t_{ag}$ , and the magnet thickness,  $t_m$  are both monotonically increasing in  $f$  across the design space and so by MP1  $g_5$  must be active bound the function from below. As there are no other constraints on these variables we can simplify the problem using equality constraints equal to their respective lower bound values. This reduces the design space to only 6 dimensions. MP2 is satisfied as all non-objective variables are constrain above and below by equality constraints ( $h_1$  through  $h_8$ ).

## 3 Optimisation in MATLAB

To find an optimal design, two different MATLAB optimisation algorithms were used, and the results compared. As the objective function is smooth and differentiable, gradient based methods were employed to find an optimum.

### 3.1 GA-SQP pipeline

First, a GA - SQP pipeline (Genetic Algorithm and Sequential Quadratic Programming) was used. GA is used to explore the design space efficiently using stochastic processes, which allow it to avoid local minima more effectively. The resultant design is then a strong initial point for the SQP algorithm to work from, exploiting the design space topology to find a local optima. It is expected that GA will produce a point within the basin of attraction of the global optima. The design defined by this is achieved a motor mass of 46.51g while successfully meeting all constraints. The

design achieved by only using GA varies but, for one run, was 49.14g - demonstrating that GA is not guaranteed to find an optima.

### 3.2 Global Search

Secondly, the MATLAB GlobalSearch function was used. This repeatedly runs solvers across the design space to find the global optima - for this particular optimisation it requires between 12 and 48 solvers in order to find the global minima. While this method is much more likely to find the global optima it comes at a cost of being much slower to run. This was used to verify the result gained from the GA-SQP pipeline. The design achieved was a motor of mass 46.51g - exactly the same as the previous design.

## 4 Conclusion

Overall, the optimisation of the motor would require further detail to provide a sufficiently robust design however serves as a good initial point for motor prototyping. The weight estimated likely higher than could be achieved as it doesn't consider optimising the part geometry beyond affecting the height and radius. However the performance of the motor regarding the torque produced and the power output are likely optimistic due to the model not considering hysteresis or cogging losses as well as ignoring magnetic saturation.

The optimum design produced by each of the algorithms used is shown in Table 2.

Algorithm	GA	SQP	Global Search
$n_w$	5.0000	5.4280	5.4280
$n_t$	3.0000	3.1059	3.1059
$w_t$ /mm	2.8661	2.0000	2.0000
$h_s$ /mm	10.0029	10.0000	10.0000
$r_s$ /mm	15.5412	14.8293	14.8293
$r_w$ /mm	0.8611	0.8815	0.8815
$t_{ag}$ /mm	0.4000	0.4000	0.4000
$t_m$ /mm	2.0000	2.0000	2.0000
Motor Mass /g	49.14	46.51	46.51

Table 2: Optimum designs produced by GA, SQP and Global Search

## References

- [1] ANNETT FA. Chapter 6: Synchronous Machines, Steady State. In: Electrical Machinery Third editionM. 3rd ed. New York: McGraw-Hill Book Co.; 1950. p. 283–329. (McGRAW HILL Electrical and Electronic Engineering series).

## 5 Nomenclature

Symbol	Meaning
$m_{motor}$	Mass of the motor
$n_w$	Number of windings per tooth
$n_t$	Number of teeth per phase
$w_t$	Tooth width
$h_s$	Stator height
$r_s$	Stator radius
$r_w$	Radius of winding wire
$t_{ag}$	Thickness of air gap
$t_m$	Thickness of magnets
$I_{max}$	Maximum current draw from battery
$V$	Battery voltage
$\tau_{cruise}$	Torque required drive propeller to move drone at $5ms^{-1}$
$\omega_{cruise}$	Angular velocity required by propeller to move drone at $5ms^{-1}$
$m_\tau$	Maximum torque as a multiple of $\tau_{cruise}$
$\beta_0$	Surface remanence of N42 neodymium magnets
$m_t$	Mass of stator teeth
$m_w$	Mass of windings
$m_{mag}$	Mass of permanent magnets
$m_r$	Mass of rotor
$m_c$	Mass of can
$\theta$	Angle given to one tooth
$R_w$	Total winding resistance
$I_{op}$	Maximum operating current based on battery and wire radius
$cyl(r, h, \rho)$	Utility function that calculates mass of a cylinder of material
$hcyl(r_i, r_o, h, \rho)$	Utility function that calculates mass of a hollow cylinder of material
$\rho_{li}$	Density of laminated iron
$\rho_c$	Density of copper
$\rho_m$	Density of neodymium
$\rho_{ms}$	Density of magnet steel
$\rho_a$	Density of aluminium
$\beta_s$	Magnetic field strength at the stator
$F$	Force generated by current moving through a magnetic field
$L$	Vector of the length of wire carrying current
$P_{losses}$	Power expended through losses

Table 3: Nomenclature of Motor Subsystem

Symbol	Meaning
BLDC	Brushless DC motor - a type of synchronous electric motor
GA	Genetic Algorithm
SQP	Sequential Quadratic Programming
MP1	Monotonicity Principle 1: In a well -constrained minimisation problem, every increasing variable is bounded below by at least one non-increasing active constraint.
MP2	In a well -constrained minimisation problem every relevant nonobjective variable is bounded both below and above.

Table 4: Nomenclature of Motor Subsystem Continued